

Adenovirus-Mediated *FLT1*-Targeted Proapoptotic Gene Therapy of Human Prostate Cancer

Sergey A. Kaliberov,¹ Lyudmila N. Kaliberova,¹ Cecil R. Stockard,²
William E. Grizzle,² and Donald J. Buchsbaum^{1,*}

¹Department of Radiation Oncology and ²Department of Pathology, University of Alabama at Birmingham, Birmingham, AL 35294, USA

*To whom correspondence and reprint requests should be addressed. Fax: +1 205 975 7060. E-mail: djb@uab.edu.

Available online 2 October 2004

Tumor necrosis factor-related apoptosis-inducing ligand (TRAIL/Apo2L) is of particular interest in the development of prostate carcinoma therapeutics as it preferentially induces apoptosis of tumor cells. To employ adenoviral vectors for highly efficient and specific *TRAIL* gene transfer into cancer cells could overcome some potential problems for recombinant TRAIL. The vascular endothelial growth factor receptor FLT-1 is involved in regulation of angiogenesis and tumor growth, invasion, and metastasis of prostate carcinoma. FLT-1 expression is observed in both tumor endothelial cells and prostate cancer cells. We developed an adenoviral vector encoding the *TRAIL* gene under control of the *FLT1* promoter (AdFlt-TRAIL), which produced endothelial and prostate cancer cell death. The combination of ionizing radiation and adenovirus-driven TRAIL expression overcame human prostate cancer cell resistance to TRAIL. Furthermore, *in vivo* administration of AdFlt-TRAIL at the site of tumor growth in combination with radiation treatment produced significant suppression of the growth of DU145 human prostate tumor xenografts in athymic nude mice. Our results suggest that specific TRAIL delivery employing the *FLT1* promoter can effectively inhibit tumor growth and demonstrate the advantage of combination radiotherapy and gene therapy for the treatment of prostate cancer.

Key Words: antiangiogenesis gene therapy, prostate cancer, TRAIL, radiation, FLT-1, adenoviral vector

INTRODUCTION

Prostate cancer is the most frequently diagnosed, non-cutaneous neoplasm and second to lung cancer in cancer-related deaths [1]. Thus, surgical, radiation, or hormonal therapy as monotherapy or in combination does not appear to be adequate to control prostate cancer, which ultimately leads to distant metastasis and morbidity [2]. Because androgen-independent prostate cancer cells eventually lead to death, successful strategies to modify the biological behavior of these cells may potentially have the most significant clinical impact [3]. Clearly other novel treatment approaches to advanced/recurrent disease are desperately needed to achieve long-term local control and particularly to develop effective systemic therapy for metastatic prostate cancer [4].

The interaction between tumor cells and their microenvironment is a promising area for the development of novel therapeutic anti-cancer modalities.

The formation of new blood vessels is an important step in prostate cancer progression. The angiogenic switch occurs early in tumorigenesis and allows for expansion of the tumor mass, favoring acquisition of additional malignant properties and metastatic dissemination [5]. In prostate cancer, the degree of tumor vascularization correlates with the development of metastatic disease. The newly formed tumor vasculature remarkably differs from mature vessels in normal tissues. Observations of human cancers and animal models argue that vascular endothelial growth factor (VEGF) receptors are up-regulated in new blood vessels [6]. A variety of studies have shown that overexpression of VEGF and its cognate receptor FLT-1 and KDR occurs in various types of tumors, in contrast to low levels in normal tissues [7]. VEGF has been implicated in the angiogenesis and growth of prostate carcinoma [8]. Recently, VEGF receptor expression was demonstrated not only in microvascu-

lar cells but also in a variety of tumor cells, including prostate carcinoma [9,10].

Antiangiogenesis therapy is a particularly attractive antitumor modality with many potential targets, considering that the regulation of tumor angiogenesis is profoundly multifactorial. Strategies to inhibit tumor angiogenesis include targeting molecules involved in blood vessel formation, as well as targeting endothelial cell survival [11]. Gene therapy is a promising approach for the treatment of prostate carcinoma. Recombinant adenoviral vectors are effective tools for gene delivery because of their superior *in vivo* gene transfer efficiency in a wide spectrum of both dividing and nondividing cell types. The employment of gene therapy using antiangiogenesis genes has shown promise in preclinical models in mice [12]. The most important obstacles for adenoviral gene therapy are low selectivity of the existing vectors and low efficiency of gene transfer. Thus, new strategies for targeting regional or systemic disease are required. The use of targeted viral vectors to localize gene transfer to specific cell types holds many advantages over conventional, nontargeted vectors currently used in gene therapy. Utilization of tumor/tissue-specific promoters can reduce toxicity, increase safety, and improve the therapeutic index [13]. Recent studies have demonstrated promising results using the *FLT1* promoter in gene therapy. Furthermore, the *FLT1* promoter exhibits a "liver off" phenotype when used in adenoviral vectors [14].

Clonal expansion and tumor growth are the result of the deregulation of the balance between cell proliferation and apoptosis. This imbalance is a major factor in the multistep process of tumorigenesis, and inhibition of apoptosis is the main cause of this phenomenon. Thus, specific induction of programmed cell death is a rational approach for cancer therapy. The extrinsic pathway of apoptosis can be induced by members of the tumor necrosis factor (TNF) family of cytokines, which includes the TNF-related apoptosis-inducing ligand (TRAIL/Apo2L) [15]. TRAIL is of particular interest in the development of cancer therapeutics as it preferentially induces apoptosis of tumor cells, with little or no effect on normal cells [16]. TRAIL can trigger caspase activation and result in rapid apoptosis through binding of specific proapoptotic receptors [17].

Induction of cytotoxicity via selective expression of the proapoptotic *TRAIL* gene in tumor microvasculature and prostate cancer cells may improve antitumor therapy alone and in combination with radiation therapy of prostate cancer xenografts. The central hypothesis of this study was that selective transcriptional targeting of adenoviral vectors encoding the *TRAIL* gene under control of the *FLT1* promoter could increase specificity and efficiency of human prostate cancer therapy in combination with ionizing radiation. The results of the present study demonstrated that overexpression of the

apoptosis-inducing *TRAIL* gene in combination with ionizing radiation may be an effective approach for the treatment of prostate cancer.

RESULTS AND DISCUSSION

FLT1 Promoter Activity in Prostate Cancer Cell Lines

Development of efficient and selective gene therapy vectors for cancer cells will increase the efficacy and safety of gene-based cancer therapeutics. Transcriptional targeting could add a further level of safety to regulate transgene expression selectively in target cells by using specific promoters for gene therapy. Ideally, promoters should provide high-level transgene expression in tumor cells but be silent in normal tissues, particularly hepatocytes. In an attempt to enhance the selectivity for prostate cancer gene therapy several adenoviral vectors were developed using well-characterized prostate cancer-specific promoters such as PSA and PSMA (for more details see reviews [18,19]). Over the past decades, numerous studies have demonstrated the importance of tumor angiogenesis in cancer development. High levels of VEGF production in prostate cancer cells and robust expression of its cognate receptors in tumor-associated blood microvessels as well as prostate carcinoma suggest that VEGF/VEGF receptor expression plays an important role in prostate tumor angiogenesis [6,7,9,10]. Recently, a fragment of the promoter for the VEGF receptor gene *FLT1* has been demonstrated to be transcriptionally silent in human hepatocytes *in vitro* and mouse and rat hepatocytes *in vivo* [20,21].

To evaluate the ability of the *FLT1* promoter to drive cell-specific gene expression, we performed an analysis of β -galactosidase production from AdFlt-LacZ adenovirus infection. Since the efficiency of gene transfer differs between cell types, we normalized infectivity for each cell type to a positive control, *LacZ* gene delivery driven by the CMV promoter (AdCMV-LacZ). This normalization is expressed as a ratio of the transfection effectiveness of AdFlt-LacZ to AdCMV-LacZ, where transfection efficiency is defined as the percentage of cells expressing *LacZ* out of the entire population. Forty-eight hours after AdFlt-LacZ or AdCMV-LacZ infection, we harvested the cells and analyzed β -galactosidase activity by β -galactosidase enzyme assay (Fig. 1A). As expected, the highest levels of *FLT1*-driven *LacZ* expression were observed in HUVEC human and SVEC4-10 murine endothelial cells and were relatively high in hormone-independent DU145 (p53-mutant) and PC3 (p53-negative) human prostate cancer cells in comparison with normal human bronchial epithelial BEAS-2B cells.

Transcriptional activity of cell-specific promoters typically correlates with the level of expression of the corresponding endogenous gene. Thus, we hypothesized that the activity of the *FLT1* promoter would correlate with the relative levels of *FLT1* mRNA expression in the

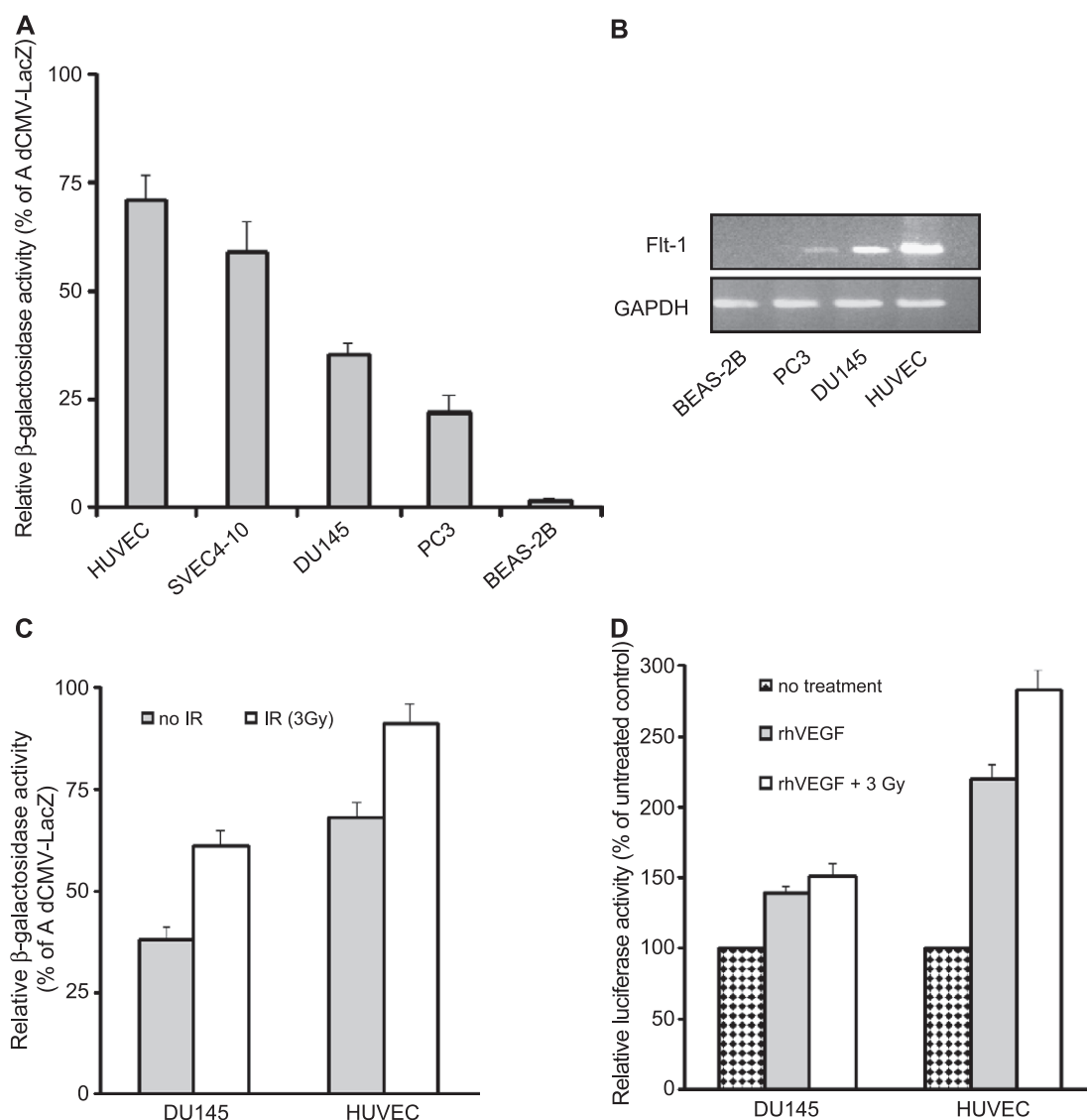


FIG. 1. *FLT1* promoter activity in prostate cancer and endothelial cells. (A) LacZ expression in prostate cancer and endothelial cell lines. DU145 and PC3 human prostate cancer cells, BEAS-2B normal human bronchial epithelial cells (negative control), SVEC4-10 small vessel murine endothelial cells, and HUVEC human umbilical vein endothelial cells (positive control) were infected with AdFlt-LacZ or AdCMV-LacZ (control for infectivity) recombinant adenoviruses at an m.o.i. of 100. LacZ expression was analyzed at 48 h after infection using a β -galactosidase enzyme assay system. *FLT1* promoter activity is presented as a percentage of CMV promoter activity. Presented are mean values \pm standard deviations of three independent experiments, each performed in triplicate. (B) The levels of *FLT1* mRNA in prostate cancer cells and endothelial cells. BEAS-2B (negative control), PC3, and DU145 prostate cancer cells and HUVEC (positive control) were collected and total RNA was extracted. The levels of *FLT1* and *GAPDH* (loading control) expression were determined using RT-PCR. One representative of three different experiments is shown. (C) Enhanced *FLT1* promoter activity following ionizing radiation treatment of human prostate cancer and endothelial cells. DU145 prostate cancer cells and HUVEC endothelial cells were infected with the AdFlt-LacZ or AdCMV-LacZ (control) recombinant adenoviruses at an m.o.i. of 100. At 24 h after infection, cells were ^{60}Co irradiated at 3 Gy. LacZ expression was analyzed at 48 h after radiation treatment using a β -galactosidase enzyme assay system. *FLT1* promoter activity is presented as a percentage of CMV promoter activity. Presented are mean values \pm standard deviations of three independent experiments, each performed in triplicate. (D) VEGF overexpression increases *FLT1* promoter activity. DU145 and HUVEC cells were infected with an m.o.i. of 100 AdFlt-Luc or AdCMV-Luc recombinant adenoviruses. Twenty-four hours later cells were exposed to ionizing radiation at 3 Gy. Immediately after radiation treatment 50 ng/ml rhVEGF was added to the cell culture medium. After 48 h incubation, cells were collected and relative luciferase activity was determined using a luciferase assay. Presented are mean values \pm standard deviations of four independent experiments, each performed in six replicates.

tested cell lines. We assessed *FLT1* and glyceraldehyde-3-phosphate dehydrogenase (*GAPDH*) (as control) mRNA levels by reverse transcriptase polymerase chain reaction

(RT-PCR). The comparative levels of the LacZ expression of prostate cancer cells correlated with VEGF receptor mRNA expression. DU145 prostate cancer cells demon-

strated detectable levels of *FLT1* mRNA expression in comparison with BEAS-2B control cells, whereas PC3 cells showed a low level *FLT1* mRNA expression (Fig. 1B). Comparing the *FLT1* promoter with CMV promoter-driven reporter expression, the specificity of the *FLT1* promoter for HUVEC endothelial cells and prostate cancer cells was demonstrated.

Ionizing radiation has an important role in localized prostate cancer treatment. Identification of compounds that will enhance the efficacy of radiation treatment is an essential goal for multimodality therapy. We further sought to determine whether ionizing radiation alters *FLT1* promoter activity. Radiation treatment at 3 Gy increased LacZ expression driven by the *FLT1* promoter by 61% in DU145 prostate cancer cells and 34% in HUVEC endothelial cells *in vitro* (Fig. 1C). Studies with a number of tumors have identified both *FLT1* and *VEGF* gene expression in malignant cells, suggesting the presence of an autocrine stimulatory loop promoting tumor cell growth in addition to the more commonly recognized effects of VEGF on tumor angiogenesis. Additionally, exposure of prostate cancer to ionizing radiation increased the secretion of VEGF by tumor cells that may enhance the angiogenic response and play a role in the protection against radiation damage [22].

To test whether VEGF protein expression modulates *FLT1* promoter activity in combination with ionizing radiation, we infected DU145 prostate cancer cells and HUVEC cells with AdFlt-Luc adenoviral vector, exposed them to ionizing radiation, and incubated them with recombinant human VEGF (rhVEGF). As shown in Fig. 1D, incubation in the presence of rhVEGF alone and in combination with radiation treatment significantly increased ($P < 0.05$) *FLT1*-driven Luc expression in HUVEC endothelial cells (220 and 282%, respectively) in comparison with AdFlt-Luc-infected DU145 prostate cancer cells (139 and 151%). These data provide evidence of relatively high levels of *FLT1* promoter activity in human endothelial cells and prostate cancer cells *in vitro*.

Tumor growth is critically dependent on blood supply and cancer cells can induce the formation of new blood vessels. Increased angiogenic activity, based on microvessel density counts of preserved tissues, has been linked to a more aggressive phenotype in studies of human prostate cancer [23,24]. High levels of VEGF have been observed in aggressive variants of human prostate cancer lines in comparison to less malignant variants [25]. Increased levels of VEGF were also identified specifically in patients with metastatic prostate cancer in comparison to prostate cancer patients with localized disease [26]. These observations indicate that increased production of VEGF may be associated specifically with the emergence of an aggressive phenotype in prostate cancer progression. Studies in model systems have shown that high levels of VEGF are likely to promote angiogenesis through paracrine mediation of endothelial cell migration and

proliferation. Recent studies of prostate carcinoma have shown that FLT-1 was detected in carcinoma cells in 100% of the specimens evaluated. FLT-1 was also expressed in benign areas adjacent to the tumors [9,10].

Although it was assumed that the two VEGF receptors are expressed almost exclusively on vascular endothelial cells, recent studies have demonstrated both KDR and FLT-1 expression in tumor cells, including those derived from neuroblastoma and prostate and pancreatic cancers [9,10,27]. In this study, we used DU145 and PC3 cell lines, which were derived from brain and bone metastases, respectively, and thus these cells would be expected to be differentiated prostate cancer cells. This agrees with observations that VEGF receptor expression is increased in prostate intraepithelial neoplasia and malignant cells from well and moderately differentiated prostate cancer, in comparison with normal glands and poorly differentiated cancer [28].

The results of our experiments are in an agreement with these findings and suggest the possibility that tumor cell-derived VEGF might play an autocrine role in prostate cancer spread in addition to its known paracrine activity. Also, VEGF overexpression and ionizing radiation increased *FLT1* promoter activity in prostate carcinoma. According to current literature, these data are the first demonstration of the ability of ionizing radiation to increase *FLT1* promoter activity.

Induction of Proapoptotic TRAIL Protein Overexpression Causes Prostate Cancer Cell Death

Failure to undergo programmed cell death has been implicated in tumor development and resistance to prostate cancer therapy [29]. Promotion of apoptosis in prostate cancer cells may lead to the regression and improved prognosis of refractory disease. Apoptosis can be achieved through the exploitation of certain cellular pathways such as death receptors and caspases. TRAIL is able to induce p53-independent apoptosis in a variety of tumor cell types, and it appeared not to induce toxicity in normal cells [30].

To determine the susceptibility of cells to TRAIL-mediated killing, we incubated DU145 and PC3 prostate cancer cells and HUVEC endothelial cells with soluble TRAIL (sTRAIL) at various concentrations and measured relative cell viability using the crystal violet staining assay (Fig. 2A). The results reveal that prostate cancer cells were resistant to sTRAIL protein. Cell viability of DU145 and PC3 cells, following incubation for 96 h with sTRAIL at 400 ng/ml, was 75 and 77%, respectively. HUVEC endothelial cells demonstrated a high level of resistance to sTRAIL treatment. Several potential problems for sTRAIL as an anti-cancer agent have been identified. Large amounts of sTRAIL were required to inhibit tumor development, as most of the protein was cleared within several hours after intravenous injection in murine models. Furthermore, the antitumor activity of sTRAIL

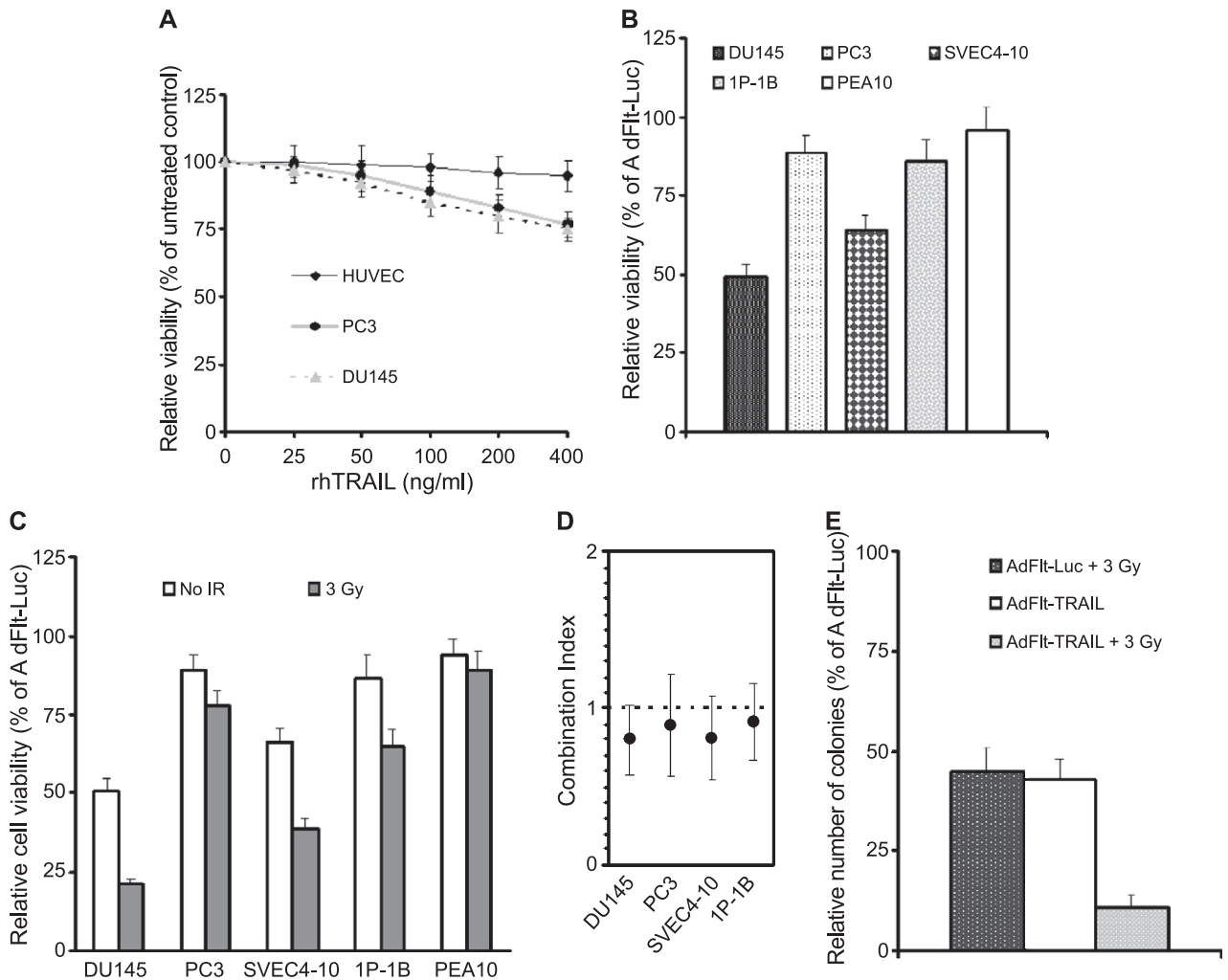


FIG. 2. Induction of proapoptotic TRAIL overexpression causes prostate cancer cell death. (A) Prostate cancer cells are resistant to sTRAIL. DU145 and PC3 prostate cancer cells and HUVEC were incubated with sTRAIL at various concentrations. Cell viability was determined at 72 h by using the crystal violet staining assay. Presented are mean values \pm standard deviations of three independent experiments, each performed in 10 replicates. (B) AdFit-TRAIL infection induces cytotoxicity in prostate cancer cells and endothelial cells. DU145 and PC3 human prostate cancer cells, SVEC4-10 and 1P-1B mouse endothelial cells, and PEA10 normal fibroblasts were infected with AdFit-TRAIL or AdFit-Luc recombinant adenoviruses at an m.o.i. of 100. Cell viability was determined at 72 h by using the crystal violet staining assay. Data shown represent relative cell viability following AdFit-TRAIL infection compared to AdFit-Luc viral control. Presented are mean values \pm standard deviations of three independent experiments, each performed in 10 replicates. (C) Induction of TRAIL expression combined with ionizing radiation resulted in increased prostate cancer cell death. Prostate cancer cells, endothelial cells, and fibroblasts were infected with AdFit-TRAIL or AdFit-Luc (viral control) recombinant adenoviruses at an m.o.i. of 100. At 24 h after infection, cells were ^{60}Co irradiated at 3 Gy. Cell viability was determined at 96 h after radiation treatment using the crystal violet staining assay. Presented are mean values \pm standard deviations of three to four independent experiments, each performed in 10 replicates. (D) Mean combination index values for AdFit-TRAIL infection and radiation treatment combinations with human prostate cancer and mouse endothelial cell lines. DU145, PC3, SVEC4-10, and 1P-1B cells were treated with different m.o.i. of AdFit-TRAIL or AdFit-Luc and 24 h later cells were irradiated at different doses. The m.o.i. of AdFit-TRAIL and AdFit-Luc ranged from 12 to 400 TCID₅₀ per cell, and the radiation dose ranged from 1 to 6 Gy. Mean values were derived from three replicate dose ranges sufficient to inhibit growth of tested cells by 5–95%. Error bars indicate the 95% confidence intervals of the mean value. Combination index values were derived from parameters of the median effect plots, and statistical tests were used to determine whether the mean combination index values at multiple effect levels (IC₅–IC₉₅) were significantly different from combination index values equal to 1. (E) Clonogenic survival assay of DU145 prostate cancer cells. AdFit-TRAIL- or AdFit-Luc-infected cells (m.o.i. of 50) were exposed to ionizing radiation at 3 Gy. Cells were fixed and colonies were counted at 15 days after radiation treatment. Data are presented as percentage of number of colonies in comparison with AdFit-Luc-infected mock-irradiated controls. Presented are mean values \pm standard deviations of three independent experiments, each performed in 6 replicates.

was highest when given shortly after tumor implantation [31,32]. Also, the reported cytotoxicity against normal human hepatocytes of some forms of sTRAIL could limit

the effectiveness of this anti-cancer agent [33,34]. Because of these issues, the development of alternative approaches to specific TRAIL protein delivery may

increase specificity and efficacy of treatment. One way to overcome these limitations is to employ adenoviral vectors for highly efficient and specific TRAIL gene transfer into cancer cells *in vitro* and *in vivo* [34–36].

We constructed a replication-deficient recombinant adenoviral vector encoding the human TRAIL gene under control of the human *FLT1* promoter element (AdFlt-TRAIL). We detected TRAIL protein expression following AdFlt-TRAIL infection in cell lysates using an immunoblotting technique (data not shown). To determine the susceptibility of prostate cancer cell and endothelial cell lines to TRAIL-mediated killing, we infected cells with AdFlt-TRAIL and AdFlt-Luc at various multiplicities of infection (m.o.i.). There was a dose-dependent correlation in cell killing measured by crystal violet staining assay (results not shown). A major advantage of using AdFlt-TRAIL would be transcriptional targeting of TRAIL gene expression in FLT-1-positive endothelial cells. Therefore, it was critical to determine whether murine endothelial cells would be sensitive to AdFlt-TRAIL infection before examining the effects of *FLT1*-driven TRAIL gene therapy *in vivo*. We infected prostate cancer cells, murine endothelial cells, and fibroblasts with AdFlt-TRAIL or AdFlt-Luc at an m.o.i. of 100 and determined cell viability using the crystal violet staining assay (Fig. 2B). AdFlt-TRAIL produced increased cytotoxicity to DU145 cells ($P < 0.05$) in comparison with the PC3 cell line. SVEC4-10 murine endothelial cells were sensitive to AdFlt-TRAIL infection, in contrast to the 1P-1B mouse endothelial cell line and PEA10 normal mouse fibroblasts. Thus, treatment using the TRAIL gene driven by the *FLT1* promoter produced prostate cancer and endothelial cell killing. Several studies recently demonstrated that adenoviral-driven TRAIL gene expression can overcome an impaired response to sTRAIL, with induction of cytotoxicity and apoptotic bystander effects in lung, colon, ovary, and prostate cancer cells [37–39]. However, the transduction of primary human hepatocytes revealed a high number of apoptotic cells [40]. These data imply that adenoviral-driven TRAIL administration *in vivo* must be restricted to tumor tissue and controlled by a specific promoter to avoid liver damage in human trials.

Additive Effect of TRAIL Overexpression in Combination with Ionizing Radiation in the Production of Prostate Cancer Cell Death

Surgical extirpation and external beam radiotherapy are potentially curative treatment options for clinically localized prostate cancer. The development of new therapeutic strategies for the treatment of hormone refractory metastatic prostate cancer is imperative. It appears that a combination treatment approach will be required to control metastatic disease. Combined radiotherapy and gene therapy is a novel therapeutic approach for prostate cancer [41,42].

To test whether combined TRAIL expression and treatment with ionizing radiation can increase cytotoxicity, we infected DU145 and PC3 human prostate cancer cells and SVEC4-10 and 1P-1B murine endothelial cells with AdFlt-TRAIL or AdFlt-Luc (as control) adenoviruses and exposed them to ionizing radiation. As shown in Fig. 2C, irradiation produced increased AdFlt-TRAIL cytotoxicity to DU145 cells ($P < 0.05$) in comparison to the PC3 cell line. Treatment with radiation enhanced the AdFlt-TRAIL-induced SVEC4-10 and 1P-1B endothelial cell killing in comparison with PEA10 normal fibroblasts (Fig. 2C), and the cytotoxic effect improved as the m.o.i. of AdFlt-TRAIL was increased (data not shown).

As shown in Fig. 2D, the combination of AdFlt-TRAIL infection with ionizing radiation treatment of prostate cancer cells and mouse endothelial cells resulted in combination index values of 0.80, with a confidence interval (CI_{95%}) from 0.58 to 1.02 and P value (indicates level of statistical significance compared with a combination index value of 1.0) of 0.05 for DU145, 0.89 (CI_{95%} = 0.46 to 1.32, $P = 0.41$) for PC3, 0.81 (CI_{95%} = 0.54 to 1.08, $P = 0.06$) for SVEC4-10, and 0.91 (CI_{95%} = 0.67 to 1.15, $P = 0.46$) for 1P-1B cells. The mean combination index values, resulting from separate experiments at multiple effect levels, were not significantly different from 1.0, which indicates an additive effect of the combined therapy for these cell lines (Fig. 2D).

We confirmed the additive interaction observed between AdFlt-TRAIL infection and radiation treatment in DU145 cells using a long-term clonogenic survival assay. The day after infection with an m.o.i. of 50 AdFlt-TRAIL or AdFlt-Luc (viral control), we exposed DU145 prostate cancer cells to ionizing radiation and subjected them to clonogenic survival assay. Radiation alone caused a dose-dependent reduction in cell survival of uninfected cells (results not shown). AdFlt-Luc-infected DU145 cells showed a reduction in the number of colonies by 55% after 3 Gy in comparison with unirradiated cells and AdFlt-TRAIL-infected cells had a 57% reduction in the number of colonies in comparison with AdFlt-Luc-infected cells (Fig. 2E). There was a significantly greater reduction ($P < 0.05$) in the number of AdFlt-TRAIL-infected DU145 colonies (89% after 3 Gy) in comparison with AdFlt-Luc-infected cells. Thus, treatment with AdFlt-TRAIL and radiation enhanced cell killing, and the cytotoxic effect improved as the m.o.i. of AdFlt-TRAIL was increased (data not shown). Combination treatment with ionizing radiation and specific proapoptotic gene transfer, two therapies with different toxicity profiles, has several potential benefits. Gene therapy may cause radiosensitization and enhanced cell killing [43]. Theoretical mechanisms of the enhanced antitumor effects from this combined approach may be that ionizing radiation improves transfection or transduction of a therapeutic gene [44]. On the other hand, radiation treatment may enhance the efficacy of TRAIL-

induced apoptosis through up-regulation of death receptor expression and/or p53-mediated transcriptional activation of Bax, Bak, or similar proapoptotic Bcl-2 family members [45].

To confirm that the tumor cell killing following AdFlt-TRAIL infection was mediated through an apoptotic mechanism, we analyzed caspase-like activity and alteration of cell membrane (Table 1). We detected increased caspase-3-like activity in the ionizing radiation-treated DU145 cells, AdFlt-TRAIL-infected DU145 cells, and cells that received combined treatment, which in comparison with AdFlt-Luc-infected cells were 3.6-, 5.3-, and 8.1-fold greater, respectively. Since caspase-3 and -7 share the same target substrate sequence, it is difficult to assess the cleavage activity attributed to caspase. The activation of caspases is the hallmark of apoptosis. The initiator caspases-8 and -9 are activated by two alternative pathways and thereby activate downstream, effector caspase-3. This caspase is ultimately involved in proteolytic cleavage of a variety of cellular proteins that leads to apoptotic cell death [46].

The loss of plasma membrane asymmetry is an early event in apoptosis and could result in the exposure of phosphatidylserine residues at the outer plasma membrane leaflet. Annexin V, a phospholipid binding protein, specifically binds to phosphatidylserine residues. The results from an annexin V-FITC binding assay showed that the higher proportion of annexin V-positive cells was observed in both AdFlt-TRAIL-infected and AdFlt-TRAIL plus radiation-treated groups, with values of 38 and 61%, respectively. These values were statistically greater than in AdFlt-Luc-infected or ionizing radiation-treated cells alone ($P < 0.05$) (Table 1). Additionally, DU145 prostate cancer cells showed an increased percentage of necrotic (propidium iodide (PI)-positive) cells following combined AdFlt-TRAIL infection and radiation treatment (data not shown).

These data demonstrated that AdFlt-TRAIL produced cytotoxicity in endothelial and prostate cancer cells through activation of the apoptosis pathway. Also, AdFlt-TRAIL infection plus ionizing radiation produced additive cell killing.

TABLE 1: The effects of combined treatment with AdFlt-TRAIL and ionizing radiation on the apoptosis of DU145 prostate cancer cells

Treatment	Fluorescence intensity (DEVD-AFC)	% of annexin V-positive cells
AdFlt-Luc (control)	350 ± 140	5 ± 3
Radiation treatment (3 Gy)	1250 ± 230*	8 ± 4
AdFlt-TRAIL	1840 ± 401*	38 ± 12**
AdFlt-TRAIL + 3 Gy	2825 ± 360**	61 ± 24**

* $P < 0.05$ in comparison with AdFlt-Luc control.

** $P < 0.05$ in comparison with AdFlt-Luc control or radiation treatment alone.

Combined TRAIL Gene Delivery with Ionizing Radiation Increased Cytotoxicity to Prostate Tumor Xenografts

Multimodality therapy has been widely used in cancer treatment for enhancing efficacy, reducing toxicity, and preventing or delaying development of resistance. There is increasing evidence that certain chemotherapeutic agents and ionizing radiation synergize with TRAIL-mediated apoptosis of cancer cells [47,48]. TRAIL triggers apoptosis even in cells resistant to apoptosis in response to radiation, since ionizing radiation induces apoptosis by a pathway different from death ligands, although an overlapping set of molecules is involved [45]. Combination of both modalities has been shown to induce additive or synergistic apoptotic effects and eradication of clonogenic tumor cells. In tumors that retain some responsiveness to conventional therapy, TRAIL overexpression in combination with ionizing radiation might lead to synergistic apoptosis activation, as well as reducing the probability that tumor cells resistant to either type of agent will emerge. In tumors that have lost p53 function, death receptor targeting might help circumvent resistance to radiotherapy. In mouse models, combinations of TRAIL and certain DNA-damaging drugs or radiotherapy exerted synergistic antitumor xenograft activity [47,48].

To investigate the effects of the combination of AdFlt-TRAIL infection and ionizing radiation treatment on tumor growth *in vivo*, we injected DU145 cells subcutaneously into the flank of athymic nude mice. Before treatment, the mean tumor sizes in groups of 10–12 mice at baseline were not significantly different between treatment groups ($P > 0.05$), and the within-treatment variances were not significantly different ($P > 0.05$). The baseline mean and standard deviation for tumor sizes was $97 \pm 39 \text{ mm}^3$. We initiated *in vivo* tumor therapy on Day 0, which corresponded to 22 days post-tumor cell injection. We injected animals intratumorally with AdFlt-TRAIL or AdFlt-Luc recombinant adenoviruses on Days 0 and 7. Two groups of mice received radiation treatment at 2 Gy on Days 1 and 8. We noted an inhibition of tumor growth in groups of mice treated with AdFlt-Luc plus radiation, AdFlt-TRAIL alone, and AdFlt-TRAIL in combination with ionizing radiation versus the AdFlt-Luc-injected control group (Fig. 3A). There were no significant differences in tumor growth between groups that received AdFlt-TRAIL alone versus AdFlt-TRAIL in combination with ionizing radiation or AdFlt-Luc plus radiation treatment versus AdFlt-TRAIL alone ($P > 0.05$). Comparisons of mean tumor volumes of the AdFlt-Luc in combination with ionizing radiation treatment group versus AdFlt-TRAIL in combination with radiation showed significant differences between the groups ($P < 0.05$). This difference in tumor size was evident at day 38 and persisted for the duration of the experiment. On day 56, the average tumor size was $101 \pm 38 \text{ mm}^3$ in mice treated with AdFlt-TRAIL in

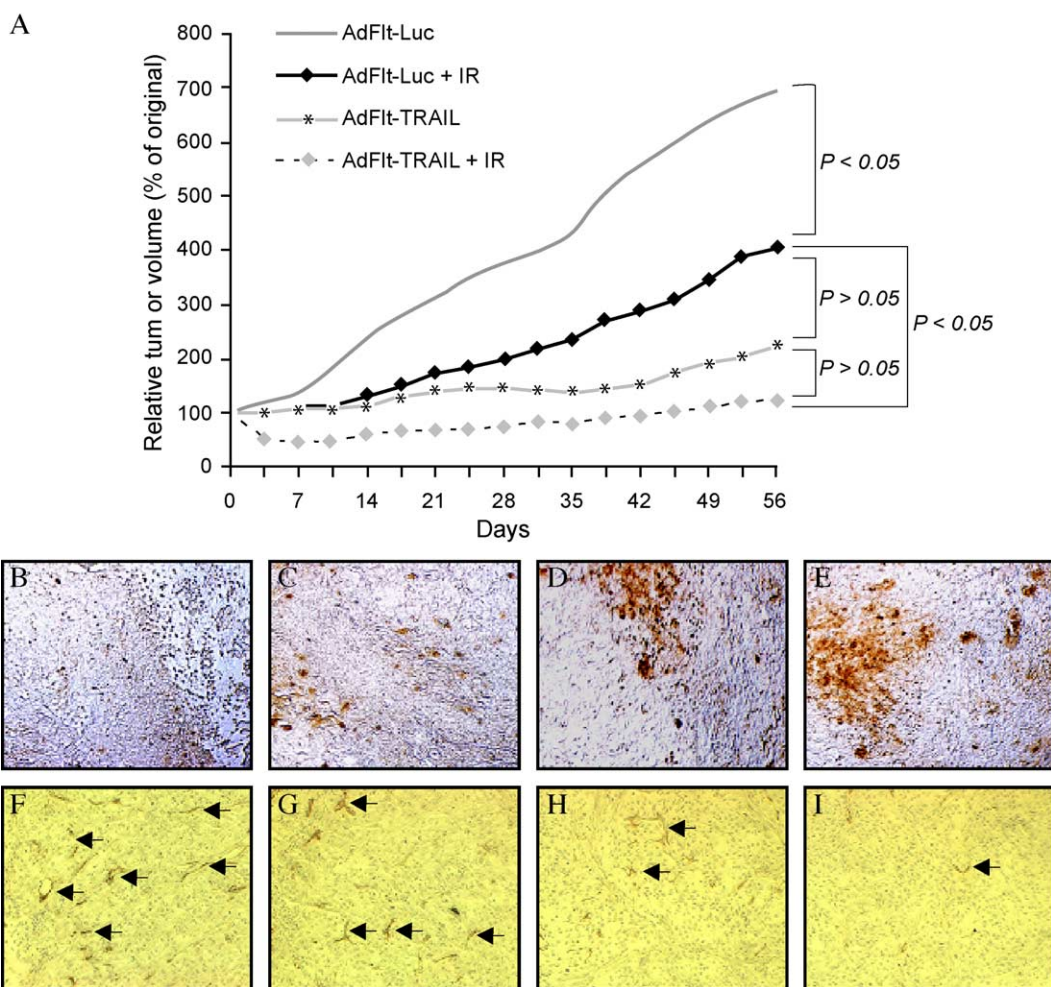


FIG. 3. The effects of AdFlt-TRAIL and radiation treatment on tumor growth in athymic nude mice bearing prostate cancer xenografts. (A) Growth of DU145 prostate cancer xenografts treated with AdFlt-TRAIL in combination with ionizing radiation. Treatment was started at the time of established tumor growth, 22 days postinjection. Animals were injected intratumorally with 1×10^9 TCID₅₀ AdFlt-TRAIL or AdFlt-Luc (control) on Days 0 and 7 and irradiated with 2 Gy on Days 3 and 9. Data points represent the mean change in tumor volume relative to Day 0 for each group of animals. On the last day of the study, the average tumor size was 101 ± 38 mm³ in mice treated with AdFlt-TRAIL in combination with ionizing radiation ($n = 10$), 193 ± 41 mm³ in mice injected with AdFlt-TRAIL alone ($n = 12$), and 368 ± 129 mm³ in mice treated with AdFlt-Luc plus radiation therapy ($n = 11$) versus 703 ± 207 mm³ in AdFlt-Luc control ($n = 12$) mice ($P = 0.015, 0.028, \text{ and } 0.04$, respectively). (B–E) TUNEL assay of DU145 prostate cancer xenografts. Representative areas of a DU145 xenograft tumor from an animal treated with AdFlt-Luc as control (B), ionizing radiation only (C), AdFlt-TRAIL alone (D), and AdFlt-TRAIL plus ionizing radiation (E). (F–I) Vascular staining in DU145 xenograft tumors. Photomicrographs of immunocytochemistry staining of tumors from nude mice with DU145 human prostate cancer xenografts, stained with an anti-CD31 antibody (arrows). Representative areas of a DU145 xenograft tumor from an animal treated with AdFlt-Luc as viral control (F), ionizing radiation alone (G), AdFlt-TRAIL alone (H), and AdFlt-TRAIL in combination with ionizing radiation (I). Original magnification $\times 200$.

combination with ionizing radiation, 193 ± 41 mm³ in mice injected with AdFlt-TRAIL alone, and 368 ± 129 mm³ in mice treated with AdFlt-Luc plus radiation therapy versus 703 ± 207 mm³ in AdFlt-Luc control mice ($P = 0.015, 0.028, \text{ and } 0.04$, respectively). The mean times to tumor doubling for control, AdFlt-Luc plus radiation, and AdFlt-TRAIL alone treatment groups were 12, 32, and 54 days, respectively; in animals that received AdFlt-TRAIL in combination with ionizing radiation tumors had not doubled by day 56, the last day of the study.

To assess the *in vivo* effects of AdFlt-TRAIL on apoptosis and angiogenesis, we analyzed the tumor samples by terminal deoxynucleotidyl transferase-mediated dUTP nick end labeling (TUNEL) and CD31 staining. DU145 xenograft-bearing mice received 2 weeks of treatment with AdFlt-TRAIL or AdFlt-Luc alone (every 7 days for three injections), radiation therapy (every 7 days for three treatments), and AdFlt-TRAIL plus radiation therapy (every 7 days for three injections plus 2 Gy the day after the adenoviral injection). At 3 days after the last

treatment, we excised the tumors, fixed them in alcoholic formalin, and stained them for apoptosis and CD31 by the procedures described under Materials and Methods. Microscopic examination of TUNEL-stained tumor sections showed that, compared to AdFlt-Luc-injected control mice (Fig. 3B) and ionizing radiation alone (Fig. 3C), AdFlt-TRAIL injection alone (Fig. 3D) or in combination with radiation (Fig. 3E) increased TdT-positive (brown-stained) cells. The quantitative evaluation of apoptosis showed that, in DU145 prostate tumor xenografts treated with AdFlt-TRAIL alone and in combination with radiation, the percentage of TUNEL-positive cells increased by 4.6- and 6.5-fold ($P < 0.05$), respectively, over that of AdFlt-Luc control tumor (Table 2). The positive control, in which TACS-nuclease was used to generate DNA fragments with free 3'-OH ends, showed positive staining in all the nuclei, whereas in the negative control, in which labeling buffer was used instead of TdT, there was not considerable positive staining (data not shown).

To determine whether the inhibitory effect of AdFlt-TRAIL on tumor growth is associated with the suppression of tumor angiogenesis, we examined the distribution of the endothelial cell-specific antigen CD31 (Table 2). The negative control, in which only blocking buffer was used instead of anti-CD31 antibody, did not show positive staining (data not shown). Immunohistochemical analysis of DU145 tumors by staining endothelial cells with anti-CD31 antibody showed fewer stained endothelial cells and reduced microvessel density ($P < 0.05$) in a cross section of tumor from mice treated with AdFlt-TRAIL alone (Fig. 3H) and AdFlt-TRAIL in combination with ionizing radiation (Fig. 3I) compared with radiation treatment alone (Fig. 3F) and AdFlt-Luc-injected tumor control (Fig. 3G), demonstrating the antiangiogenesis efficacy of AdFlt-TRAIL against endothelial cells *in vivo*.

These *in vivo* tumor therapy studies demonstrated significant inhibition of DU145 tumor growth in animals that received AdFlt-TRAIL alone and in combination with radiation treatment in comparison with PBS control tumors. Moreover, in the group treated with AdFlt-TRAIL alone (12 mice), 5 of the tumors underwent complete regression and 2 eventually recurred. In contrast, the

group treated with AdFlt-TRAIL in combination with ionizing radiation showed 3/10 regressions without recurrence.

In an attempt to improve the outcome of patients with prostate cancer, combined modality approaches are frequently considered. Combined therapy, most frequently radiosensitizing chemotherapy and radiation, has been shown to be particularly efficient and has become standard therapy for many tumor types. One of the most promising therapies that can be combined with ionizing radiation in the treatment of prostate cancer is antiangiogenic gene therapy. Angiogenesis is a critical requirement for local proliferation and metastasis in prostate cancer [49]. The tumor response to radiation is determined not only by tumor cell phenotype but also by microvascular sensitivity [50]. Inhibitors of tumor angiogenesis interrupt the angiogenic process to prevent new vessel formation. In this study, we used specifically targeted proapoptotic gene transfer to cause direct damage to the tumor endothelium and thus lead to extensive secondary tumor cell death. The application of such strategies as TRAIL expression in endothelial cells and tumor cells with conventional radiation treatments offers unique opportunities to develop more effective cancer therapies.

Our results suggest that specific TRAIL delivery employing the *FLTI* promoter can effectively inhibit tumor growth and demonstrate the advantage of combination radiotherapy and gene therapy for the treatment of prostate cancer. The *FLTI* gene is member of the VEGF/VEGF receptor family, which is extremely important for angiogenesis regulation. Neovascularization is an essential step in a number of different physiological processes. Thus, specific vascular-targeted gene therapy may be applied as a therapeutic intervention for angiogenesis regulation. For future studies of antiangiogenesis cancer treatment, specific gene therapy using recombinant AdFlt-TRAIL may help overcome the undesired neovascularization and decrease the risk of neoplastic growth and metastasis.

MATERIALS AND METHODS

Adenoviral vectors, cell culture, and reagents

A replication-deficient recombinant adenoviral vector encoding the TRAIL gene under control of the human *FLTI* promoter element (AdFlt-TRAIL) was constructed using a method reported previously [51]. Briefly, to generate pShuttleFlt-TRAIL plasmid, the fragment including TRAIL cDNA and the SV40 late polyadenylation signal was removed from the pGT60hTRAIL plasmid (InvivoGen, San Diego, CA, USA), blunted, and cloned into the *FLTI* promoter element pShuttleFlt-Luc plasmid, which was digested and from which Luc cDNA was removed prior to cloning in the TRAIL cDNA and SV40 late polyadenylation signal fragment. The insert sequence was confirmed by restriction enzyme mapping and partial sequencing analysis. The resultant plasmid was linearized and cotransfected with pAdEasy-1 plasmid (Quantum Biotechnologies, Montreal, QC, Canada). Recombinant clones were confirmed by PCR analysis, linearized, and transected into 293 cells using the Superfect lipid-based transfection method (Qiagen, Chatsworth, CA, USA) to generate AdFlt-TRAIL recombi-

TABLE 2: The effects of combined treatment with AdFlt-TRAIL and ionizing radiation on apoptosis and tumor microvessel density of DU145 prostate cancer xenografts

Treatment	TUNEL-positive cells (%)	CD31-positive vessel density/100× field
AdFlt-Luc	1.8 ± 0.8	35 ± 3.8
Ionizing radiation (2 Gy)	2.9 ± 1.2	29 ± 2.4
AdFlt-TRAIL	8.4 ± 1.5***	21 ± 1.2*
AdFlt-TRAIL + 2 Gy	11.8 ± 1.6***	11 ± 1.7***

* $P < 0.05$ in comparison with AdFlt-Luc control.

** $P < 0.05$ in comparison with radiation treatment alone.

nant adenovirus, which was isolated from a single positive plaque and passed through three rounds of plaque purification and subsequently confirmed by PCR. AdFlt-Luc (encoding the firefly luciferase gene under the control of the human *FLT1* promoter element) and AdCMV-Luc (encoding the firefly luciferase gene under the control of the human CMV promoter element) were kindly provided by Dr. P. N. Reynolds (University of Adelaide, Adelaide, SA, Australia). All viruses were propagated in 293 cells, purified by ultracentrifugation in a cesium chloride gradient, and subjected to dialysis. Viral titer was measured by a standard 50% tissue culture infectious dose (TCID₅₀) assay using 293 cells and by absorbance of the dissociated virus at A_{260} nm. Multiplicities of infection for subsequent experiments were expressed as TCID₅₀ per cell.

For this study, cell lines, except human umbilical vein endothelial cells (HUVEC), were obtained from the American Type Culture Collection (Rockville, MD, USA). The HUVEC were obtained from Clonetics (San Diego, CA, USA) and were grown in EGM-2 growth medium (Clonetics). The normal human bronchial epithelial adenovirus 12-SV40 virus hybrid-transformed BEAS-2B cells were grown in BEGM growth medium (Clonetics). The human prostate adenocarcinoma PC3 and DU145 cells, transformed small vessel murine endothelial cells SVEC4-10 and 1P-1B, and human embryonic kidney HEK293 cells were grown in Dulbecco's modified Eagle's medium (DMEM) with 10% fetal bovine serum (FBS). All cells were maintained at 37°C in a humidified atmosphere with 5% CO₂.

Human recombinant VEGF protein was purchased from Pierce (Rockford, IL, USA). The full-length TRAIL protein of human origin was provided by Santa Cruz Biotechnology (Santa Cruz, CA, USA). Rat anti-mouse CD31 PECAM-1 antibody was obtained from BD Pharmingen (San Diego, CA, USA) and secondary donkey anti-rat antibody was purchased from Jackson ImmunoResearch Laboratories (West Grove, PA, USA).

Reporter gene assays

β -Gal assay. Cells were seeded in 24-well plates in triplicate at a density of 5×10^4 cells/well. The next day, the cells were infected with AdFlt-LacZ or AdCMV-LacZ (control) at an m.o.i. of 100 in DMEM with 2% FBS for 1 h and then maintained in complete medium. For staining, wells were washed with 1 mM MgCl₂ in PBS, and cells were fixed by 0.5% (v/v) glutaraldehyde at room temperature, then stained using X-gal reaction solution, and incubated at 37°C, until a color change was obtained, and the absorbance was measured at 420 nm using a V Max plate reader (Molecular Devices Corp., Sunnyvale, CA, USA). LacZ activities were normalized for differences in incubation times.

Luciferase assay. Cells were plated in 24-well plates in triplicate at a density of 5×10^4 cells/well. The next day, the cells were infected with AdFlt-Luc or AdCMV-Luc (control) at an m.o.i. of 50 in DMEM with 2% FBS for 1 h and then maintained in complete medium. Forty-eight hours after infection cells were harvested and treated with 100 μ l of lysis buffer. A luciferase assay (Promega, Pittsburgh, PA, USA) and a FB12 luminometer (Zylux Corp., Oak Ridge, TN, USA) were used for the evaluation of luciferase activity of infected cells. Luciferase activity was normalized by the protein concentration in the cell lysate using the DC Protein Assay (Bio-Rad).

RNA preparation and RT-PCR. The levels of VEGF receptor *FLT1* messenger RNA were determined by RT-PCR. Total RNA was extracted using the RNeasy Mini Kit (Qiagen), following standard protocol, and quantified spectrophotometrically using an MBA 2000 spectrophotometer (Perkin-Elmer, Wellesley, MA, USA). cDNA was synthesized using random hexamer primers and an Omniscript RT kit (Qiagen). The first-strand cDNA was used as the template for PCR. For amplification of cDNA encoding *FLT1* the following primers were used: 5'-GAGGATTC-TGACGGTTTC-3' (3199-FLT) and 5'-CCTGTCACTATGGCATTG-3' (FLT-3782). The human *GAPDH* cDNA was used as an internal standard for template loading of PCR by using primers 5'-TCCCACCATCTTCCA-3' (*GAPDH* forward) and 5'-CATCAGCCACAGTTTCC-3' (*GAPDH* reverse). PCR was performed under the following conditions: 30 cycles of 95°C for 45 s, 55°C for 45 s, and 72°C for 1 min. PCR products were analyzed by 1% agarose electrophoresis with ethidium bromide staining.

Cell proliferation assay. The dye in this colorimetric assay is crystal violet, which is a cationic triarylmethane dye that preferentially stains DNA and allows one to obtain quantitative information about the relative density of adherent cells. Upon solubilization, the amount of dye taken up by the monolayer can be quantitated by optical density. To determine cell growth after recombinant adenovirus infection, human prostate cancer cells were seeded in 96-well plates at 5×10^3 cells/well, incubated for 24 h with or without rhVEGF, and infected at different m.o.i. with AdFlt-TRAIL or AdFlt-Luc. At 72 h after incubation cell culture medium was removed and surviving cells were then fixed and stained with 2% (w/v) crystal violet (Sigma-Aldrich, St. Louis, MO, USA) in 70% ethanol for 3 h at room temperature. The plates were washed extensively and air-dried and optical density was measured at 570 nm using a V Max plate reader (Molecular Devices Corp.). Relative density of adherent cells was defined as OD₅₇₀ of treated cells in comparison with untreated cells and the OD₅₇₀ value of blank wells was subtracted.

Clonogenic survival assay. At 3 h after infection with an m.o.i. of 50 AdFlt-TRAIL or AdFlt-Luc, cells were trypsinized and diluted to the appropriate cell density into six-well culture plates, and after 24 h incubation at 37°C cells were either mock-irradiated or irradiated at 3 Gy dose using a ⁶⁰Co γ -irradiator (⁶⁰Co Picker Unit, Cleveland, OH, USA) and were then returned to the incubator and cultured for an additional 15 days. Cells were then fixed with 70% ethanol and stained with 2% (w/v) crystal violet (Sigma-Aldrich). Colonies comprising at least 50 cells were counted. The plating efficiencies were calculated as the number of colonies divided by the number of test cells plated for each data point. Plating efficiencies were referenced back to the mock-irradiated control plating efficiency to determine the surviving fraction for each dose.

Apoptosis assays

Annexin V staining and propidium iodide uptake of apoptotic cells. Annexin V and PI double staining (BioVision, Palo Alto, CA, USA) was used to determine apoptosis. Annexin V binds to cells that express phosphatidylserine on the outer layer of the cell membrane, and PI stains the cellular DNA of cells with a compromised cell membrane. This allows for the discrimination of live cells (unstained with either fluorochrome) from apoptotic cells (stained only with annexin V) and necrotic cells (stained with both annexin V and PI). Cells were collected and double stained with FITC-conjugated annexin V and PI for 15 min at room temperature. Annexin V and PI were added according to the manufacturer's recommendations (BioVision). Samples were immediately analyzed by flow cytometry. Annexin V and PI emissions were detected in the FL-1 (530/30 nm) and FL-2 (585/40 nm) channels, respectively. For each sample, data from approximately 1×10^4 cells were recorded in list mode on logarithmic scales. Analysis was performed with CellQuest software (Becton-Dickinson, San Jose, CA, USA) on cells characterized by forward/side scatter (FSC/SSC) parameters. Cell debris characterized by a low FSC/SSC was excluded from analysis. The percentages of apoptotic cells were calculated.

Caspase protease assay. Caspase-like activity was measured using Ac-DEVD-AFC as fluorometric substrates for caspase-3 (BioVision). Total adherent and floating cells were resuspended on ice in cell lysis buffer. The protein concentration in the samples was determined by the Biuret method using the BCA Protein Assay Kit (Pierce). Fifty micrograms of cell lysate was added (1:1, v/v) to 2 \times reaction buffer containing 10 mM DTT and AFC (7-amino-4-trifluoromethyl coumarin)-conjugated substrates (50 μ M final concentration) and incubated at 37°C for 2 h. The optical density was measured in a VersaFluor fluorometer (Bio-Rad, Hercules, CA, USA) equipped with 400-nm excitation and 505-nm emission filters. The change in caspase-like activity was determined by comparing relative fluorescence of treated samples with the level of untreated controls.

In vivo tumor therapy studies

For *in vivo* experiments 8- to 10-week-old female nude mice (National Cancer Institute, Frederick Cancer Research and Development Center, Frederick, MD, USA) were subcutaneously inoculated with 5×10^6 DU145 tumor cells, which were mixed 1:1 with Matrigel (Becton-Dickinson). Treatment was started 22 days later at the time of established tumor growth (250–350 mm³). Mice were randomly divided (10–12 mice/group)

into four groups receiving different treatments: (1) AdFlt-Luc (control), (2) AdFlt-Luc and ^{60}Co radiation treatment at 2 Gy, (3) AdFlt-TRAIL, and (4) AdFlt-TRAIL and 2 Gy radiation treatment. Animals were injected intratumorally with 1×10^9 TCID₅₀ recombinant adenoviruses. Radiation treatment was administered 24 h after adenoviral injection. Tumor volume ($0.5 \times \text{length} \times \text{width}^2$ in mm³) was measured twice a week using calipers. Percentage change from baseline at 22 days was computed by comparing the baseline value to the tumor size on each day of measurement. Also, the times to death from tumor or treatment, to tumor regression, and to tumor recurrence were recorded.

In situ apoptosis detection by TUNEL staining

The formalin-fixed and paraffin-embedded 5- μm -thick sections of all tumor samples were studied by TUNEL staining by using the Apoptag Kit (Intergen, Purchase, NY, USA). The extent of apoptosis was evaluated by counting the positive brown-stained cells as well as the total number of cells at 10 arbitrarily selected fields in a blinded manner. The apoptotic index was calculated as the number of apoptotic cells per 200 \times microscope field.

Immunohistochemical analysis of tumors for CD31 expression

Sections from paraffin-embedded tumors (those used for TUNEL staining) were incubated overnight with rat anti-mouse CD31 polyclonal antibody. Then sections were incubated with donkey anti-rat antibody secondary antibody. Antigen-antibody complexes were visualized by incubation with 3,3'-diaminobenzidine substrate and counterstained with diluted Harris hematoxylin. Tumor vessels containing CD31-positive (brown) cells were quantified by microscopy in 100 \times fields (at least five random fields/tumor) and were calculated as relative vessel density.

Statistical analysis

All error terms are expressed as the standard deviation of the mean. Significance levels for comparison of differences between groups in the *in vitro* experiments were analyzed by the Student *t* test. The differences were considered significant when *P* value was <0.05. All reported *P* values are two-sided. In the animal model tumor therapy studies, the treatment groups were compared with respect to tumor size and percentage of original tumor size over time. To test for significant differences in tumor size between treatment groups, one-way analysis of variance (ANOVA) test was conducted. When the ANOVA indicated that a significant difference existed (*P* value <0.05), multiple comparison procedures were used to determine where the differences lay. Multiple drug effect analysis was performed using computer software [52]. To calculate combined AdFlt-TRAIL and ionizing radiation effects, the combination index isobologram method was used. Details of this methodology have been published previously [53]. Briefly, this method defines the expected additive effect of combined agents and then quantifies the degree of enhancement/reduction of effect by determining how much the combination effect differs from the expected additive effect using the combination index. The combination index equation takes into account both the potency and the shape of the dose-effect curves. In this analysis, synergy is defined as mean combination index values significantly less than 1.0, antagonism as mean combination index values significantly greater than 1.0, and additivity as mean combination index values not significantly different from 1.0.

ACKNOWLEDGMENT

The authors thank Sally B. Lagan for assistance in preparing the manuscript.

RECEIVED FOR PUBLICATION JUNE 8, 2004; ACCEPTED AUGUST 30, 2004.

REFERENCES

- Jemal, A., et al. (2002). Cancer statistics. *CA J. Cancer Clin.* **52**: 23–47.
- Schellhammer, P. F., and Lynch, D. F. (1997). Are monotherapy options reasonable for T3 prostate cancer? *Semin. Urol. Oncol.* **15**: 207–214.
- Isaacs, W. B. (1995). Molecular genetics of prostate cancer. *Cancer Surv.* **25**: 357–379.
- Steiner, M. S., Gingrich, J. R., and Chauhan, R. D. (2002). Prostate cancer gene therapy. *Surg. Oncol. Clin. North Am.* **11**: 607–620.
- Folkman, J. (2003). Angiogenesis and apoptosis. *Semin. Cancer Biol.* **13**: 159–167.
- Feng, D., et al. (2000). Ultrastructural localization of the vascular permeability factor/vascular endothelial growth factor (VPF/VEGF) receptor-2 (FLK-1, KDR) in normal mouse kidney and in the hyperpermeable vessels induced by VPF/VEGF-expressing tumors and adenoviral vectors. *J. Histochem. Cytochem.* **48**: 545–556.
- Dvorak, H. F., et al. (1991). Distribution of vascular permeability factor (vascular endothelial growth factor) in tumors: concentration in tumor blood vessels. *J. Exp. Med.* **174**: 1275–1278.
- Ferrer, F. A., et al. (1999). Expression of vascular endothelial growth factor receptors in human prostate cancer. *Urology* **54**: 567–572.
- Fakhari, M., et al. (2002). Upregulation of vascular endothelial growth factor receptors is associated with advanced neuroblastoma. *J. Pediatr. Surg.* **37**: 582–587.
- Soker, S., et al. (2001). Vascular endothelial growth factor-mediated autocrine stimulation of prostate tumor cells coincides with progression to a malignant phenotype. *Am. J. Pathol.* **159**: 651–659.
- Sternberg, C. N. (2003). What's new in the treatment of advanced prostate cancer? *Eur. J. Cancer* **39**: 136–146.
- Scappaticci, F. A., et al. (2001). Combination angiostatin and endostatin gene transfer induces synergistic antiangiogenic activity in vitro and antitumor efficacy in leukemia and solid tumors in mice. *Mol. Ther.* **3**: 186–196.
- St George, J. A. (2003). Gene therapy progress and prospects: adenoviral vectors. *Gene Ther.* **10**: 1135–1141.
- Nicklin, S. A., et al. (2003). Transductional and transcriptional targeting of cancer cells using genetically engineered viral vectors. *Cancer Lett.* **201**: 165–173.
- Wiley, S. R., et al. (1995). Identification and characterization of a new member of the TNF family that induces apoptosis. *Immunity* **3**: 673–682.
- Pan, G., et al. (1997). An antagonist decoy receptor and a death domain-containing receptor for TRAIL. *Science* **277**: 815–818.
- Schneider, P., et al. (1997). TRAIL receptors 1 (DR4) and 2 (DR5) signal FADD-dependent apoptosis and activate NF-kappaB. *Immunity* **7**: 831–836.
- Mabjeesh, N. J., Zhong, H., and Simons, J. W. (2002). Gene therapy of prostate cancer: current and future directions. *Endocr. Relat. Cancer* **9**: 115–139.
- Collis, S. J., Khater, K., and DeWeese, T. L. (2003). Novel therapeutic strategies in prostate cancer management using gene therapy in combination with radiation therapy. *J. World Urol.* **21**: 275–289.
- Nicklin, S. A., et al. (2001). Analysis of cell-specific promoters for viral gene therapy targeted at the vascular endothelium. *Hypertension* **38**: 65–70.
- Reynolds, P. N., et al. (2001). Combined transductional and transcriptional targeting improves the specificity of transgene expression in vivo. *Nat. Biotechnol.* **19**: 838–842.
- Abdollahi, A., et al. (2003). SU5416 and SU6668 attenuate the angiogenic effects of radiation-induced tumor cell growth factor production and amplify the direct anti-endothelial action of radiation in vitro. *Cancer Res.* **63**: 3755–3763.
- Weidner, N., et al. (1993). Tumor angiogenesis correlates with metastasis in invasive prostate carcinoma. *Am. J. Pathol.* **143**: 401–409.
- Bettencourt, M. C., et al. (1998). CD34 immunohistochemical assessment of angiogenesis as a prognostic marker for prostate cancer recurrence after radical prostatectomy. *J. Urol.* **160**: 459–465.
- Balbay, M. D., et al. (1999). Highly metastatic human prostate cancer growing within the prostate of athymic mice overexpresses vascular endothelial growth factor. *Clin. Cancer Res.* **5**: 783–789.
- Duque, J. L., et al. (1999). Plasma levels of vascular endothelial growth factor are increased in patients with metastatic prostate cancer. *Urology* **54**: 523–527.
- von Marschall, Z., et al. (2000). De novo expression of vascular endothelial growth factor in human pancreatic cancer: evidence for an autocrine mitogenic loop. *Gastroenterology* **119**: 1358–1372.
- Jackson, M. W., et al. (2002). A potential autocrine role for vascular endothelial growth factor in prostate cancer. *Cancer Res.* **62**: 854–859.
- Denmeade, S. R., Lin, X. S., and Isaacs, J. T. (1996). Role of programmed (apoptotic) cell death during the progression and therapy for prostate cancer. *Prostate* **28**: 251–265.
- Walczak, H., et al. (1999). Tumoricidal activity of tumor necrosis factor-related apoptosis-inducing ligand in vivo. *Nat. Med.* **5**: 157–163.
- Ashkenazi, A., et al. (1999). Safety and antitumor activity of recombinant soluble Apo2 ligand. *J. Clin. Invest.* **104**: 155–162.
- Lawrence, D., et al. (2001). Differential hepatocyte toxicity of recombinant Apo2L-TRAIL versions. *Nat. Med.* **7**: 383–385.
- LeBlanc, H. N., and Ashkenazi, A. (2003). Apo2L-TRAIL and its death and decoy receptors. *Cell Death Differ.* **10**: 66–75.
- Griffith, T. S., et al. (2000). Adenoviral-mediated transfer of the TNF-related apoptosis-inducing ligand/Apo-2 ligand gene induces tumor cell apoptosis. *J. Immunol.* **165**: 2886–2894.
- Griffith, T. S., and Broghammer, E. L. (2001). Suppression of tumor growth following intraliesional therapy with TRAIL recombinant adenovirus. *Mol. Ther.* **4**: 257–266.
- Lee, J., Hampl, M., Albert, P., and Fine, H. A. (2002). Antitumor activity and prolonged expression from a TRAIL-expressing adenoviral vector. *Neoplasia* **4**: 312–323.
- Huang, X., et al. (2002). Combined TRAIL and Bax gene therapy prolonged survival in mice with ovarian cancer xenograft. *Gene Ther.* **9**: 1379–1386.

38. Lin, T., *et al.* (2002). Targeted expression of green fluorescent protein/tumor necrosis factor-related apoptosis-inducing ligand fusion protein from human telomerase reverse transcriptase promoter elicits antitumor activity without toxic effect on primary human hepatocytes. *Cancer Res.* **62**: 3620–3625.
39. Lin, T., *et al.* (2002). Long-term tumor-free survival from treatment with the GFP-TRAIL fusion gene expressed from the hTERT promoter in breast cancer cells. *Oncogene* **21**: 8020–8028.
40. Armeanu, S., *et al.* (2003). Adenoviral gene transfer of tumor necrosis factor-related apoptosis-inducing ligand overcomes an impaired response of hepatoma cells but causes severe apoptosis in primary human hepatocytes. *Cancer Res.* **63**: 2369–2372.
41. Parker, C. C., and Dearnaley, D. P. (2003). Radical radiotherapy for prostate cancer. *Cancer Treat. Rev.* **29**: 161–169.
42. Teh, B. S., *et al.* (2002). Combining radiotherapy with gene therapy (from the bench to the bedside): a novel treatment strategy for prostate cancer. *Oncologist* **7**: 458–466.
43. Atkinson, G., and Hall, S. J. (1999). Prodrug activation gene therapy and external beam irradiation in the treatment of prostate cancer. *Urology* **54**: 1098–1104.
44. Stevens, C. W., Zeng, M., and Cerniglia, G. J. (1996). Ionizing radiation greatly improves gene transfer efficiency in mammalian cells. *Hum. Gene Ther.* **7**: 1727–1734.
45. Belka, C., *et al.* (2004). Apoptosis-modulating agents in combination with radiotherapy—current status and outlook. *Int. J. Radiat. Oncol. Biol. Phys.* **58**: 542–554.
46. Waxman, D. J., and Schwartz, P. S. (2003). Harnessing apoptosis for improved anticancer gene therapy. *Cancer Res.* **63**: 8563–8572.
47. Gliniak, B., and Le, T. (1999). Tumor necrosis factor-related apoptosis-inducing ligand's antitumor activity in vivo is enhanced by the chemotherapeutic agent CPT-11. *Cancer Res.* **59**: 6153–6158.
48. Chinnaiyan, A. M., *et al.* (2000). A combined effect of tumor necrosis factor-related apoptosis-inducing ligand and ionizing radiation in breast cancer therapy. *Proc. Natl. Acad. Sci. USA* **97**: 1754–1759.
49. Nicholson, B., and Theodorescu, D. (2004). Angiogenesis and prostate cancer tumor growth. *J. Cell. Biochem.* **91**: 125–150.
50. Garcia-Barros, M., *et al.* (2003). Tumor response to radiotherapy regulated by endothelial cell apoptosis. *Science* **300**: 1155–1159.
51. Kaliberov, S. A., *et al.* (2002). Adenovirus-mediated transfer of BAX driven by the vascular endothelial growth factor promoter induces apoptosis in lung cancer cells. *Mol. Ther.* **6**: 190–198.
52. Dressler, V., Muller, G., and Suhnel, J. (1999). CombiTool—a new computer program for analyzing combination experiments with biologically active agents. *Comput. Biomed. Res.* **32**: 145–160.
53. Chou, T. C., and Talalay, P. (1984). Quantitative analysis of dose–effect relationships: the combined effects of multiple drugs or enzyme inhibitors. *Adv. Enzymol. Regul.* **22**: 27–55.